Theory of Topological Quantum Phase Transitions in 3D Noncentrosymmetric Systems

Bohm-Jung Yang,[1] Mohammad Saeed Bahramy,[1] Ryotaro Arita,[1,2] Hiroki Isobe,[2]
Eun-Gook Moon,[3] and Naoto Nagaosa[1,2]

[1]*RIKEN Center for Emergent Matter Science, Wako, Saitama 351-0198, Japan*
[2]*Department of Applied Physics, University of Tokyo, Tokyo 113-8656, Japan*
[3]*Department of Physics, University of California, Santa Barbara, California 93106, USA*

(Received 8 July 2012; published 19 February 2013)

We construct a general theory describing the topological quantum phase transitions in 3D systems with broken inversion symmetry. While the consideration of the system's codimension generally predicts the appearance of a stable metallic phase between the normal and topological insulators, it is shown that a direct topological phase transition between two insulators is also possible when an accidental band crossing occurs along directions with high crystalline symmetry. At the quantum critical point, the energy dispersion becomes quadratic along one direction while the dispersions along the other two orthogonal directions are linear, which manifests the zero chirality of the band touching point. Because of the anisotropic dispersion at quantum critical point, various thermodynamic and transport properties show unusual temperature dependence and anisotropic behaviors.

DOI: 10.1103/PhysRevLett.110.086402 PACS numbers: 71.30.+h, 64.70.Tg, 71.10.Hf, 72.80.Sk

The 3D topological insulator (TI) is a new state of matter in which the nontrivial topology of bulk electronic wave functions guarantees the existence of gapless states on the sample's boundary [1,2]. Because of its topological nature, the surface gapless states are protected against small perturbations, preserving the time-reversal symmetry (TRS) as long as the bulk band gap remains finite. Therefore, to change the bulk topological property, the band gap should be closed at some points in the Brillouin zone (BZ) via accidental band crossing (ABC). Recently, such a topological phase transition (PT) is realized in $BiTl(S_{1-x}Se_x)_2$ [3,4], by modulating the spin-orbit interaction or the crystal lattice. In inversion symmetric systems such as $BiTl(S_{1-x}Se_x)_2$, the topological PT can be described by the $(3+1)$-dimensional massive Dirac Hamiltonian, in general. In this sense, the topological PT of 3D TIs provides a new venue to study intriguing quantum critical behaviors of 3D particles with relativistic dispersion [5–7].

On the other hand, for noncentrosymmetric systems, our understanding of the topological PT and of the corresponding quantum critical behavior is still incomplete. By considering the codimension for ABC, a stable metallic phase was predicted to appear between a TI and a normal insulator in 3D noncentrosymmetric systems [8]. The intervening metallic phase, dubbed a Weyl semimetal, has topological stability because there are several gapless points (Weyl points) with nonzero chiral charge at the Fermi level [9]. Therefore, before every Weyl point is annihilated by colliding with another Weyl point with opposite chiral charge, the Weyl semimetal should stably survive across the PT. In this respect, the recent discovery of a direct PT between two insulators in the noncentrosymmetric compound BiTeI is an unexpected surprise [10–12]. At the quantum critical point (QCP) of BiTeI, instead of a Weyl semimetal, several isolated band touching points (BTPs) with anisotropic dispersion appear, which suggests the diversity of the possible phase diagrams of noncentrosymmetric systems accessible via ABC.

In this Letter, we propose generic phase diagrams for 3D noncentrosymmetric systems that can be achieved through ABC, as depicted in Fig. 1. We carry out the analysis of the minimal two-band Hamiltonian describing the ABC to derive the conditions for these insulator-to-metal and insulator-to-insulator transitions (IITs). The key ingredient to obtain Fig. 1 is the fact that the chirality of the BTP at the QCP is zero. Therefore, it can either be gapped out, leading to another insulator [Fig. 1(a)], or split into several Weyl points, resulting in a Weyl semimetal. In the latter case, depending on whether the trajectory, traversed by the Weyl point, is closed or not, the Weyl semimetal phase turns into another insulator [Fig. 1(b)] or persists all the way [Fig. 1(c)]. In all three cases, at the QCP between any pair of neighboring phases, the energy dispersion near a BTP is highly anisotropic, which is linear in two directions and quadratic along the third direction. This anisotropic dispersion induces new power laws in the temperature dependence of various measurable quantities and anisotropic physical responses.

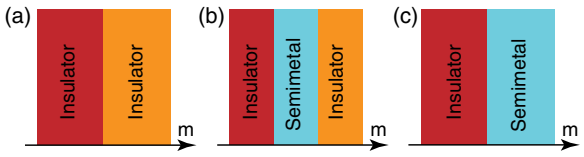

FIG. 1 (color online). Generic phase diagrams, resulting from the ABC between the conduction and valence bands in 3D noncentrosymmetric systems. Here, m indicates an external control parameter.

Phase transition through the ABC.—In noncentrosymmetric systems, the ABC between the conduction and valence bands can be described by the following 2×2 Hamiltonian, $H(\mathbf{k}, m) = f_0(\mathbf{k}, m) + \sum_{i=1}^{3} f_i(\mathbf{k}, m)\tau_i$, where $f_{0,1,2,3}$ are real functions and $\tau_{1,2,3}$ are Pauli matrices indicating the two bands. Here, m describes a tuning parameter. In particular, we consider the following situation. For $m < m_c$, the system is fully gapped. An isolated BTP occurs at the critical point $(\mathbf{k}, m) = (\mathbf{k}_c, m_c)$, where $f_{1,2,3}(\mathbf{k}_c, m_c) = 0$. Since f_0 does not affect the ABC, we can neglect f_0. Then, the next question is what happens when $m > m_c$. To examine the system's behavior near the critical point, we derive the effective Hamiltonian through an expansion in powers of $\mathbf{q} = \mathbf{k} - \mathbf{k}_c$ and $\Delta m = m - m_c$. Up to the linear order of $\mathbf{q}$ and Δm, $\mathbf{f} = (f_1, f_2, f_3)^T$ (T stands for transpose) can be written as $\mathbf{f}(\mathbf{q}, \Delta m) = \hat{M}\mathbf{q} + \Delta m \mathbf{N}$, where $\hat{M}_{ij} = \frac{\partial f_i}{\partial q_j}|_{\mathbf{q}=\Delta m=0}$ and $N_i = \frac{\partial f_i}{\partial m}|_{\mathbf{q}=\Delta m=0}$. If the determinant of $\hat{M}$, i.e., $\mathrm{Det}\hat{M}$, is nonzero, the gap-closing condition $\mathbf{f} = 0$ leads to $\mathbf{q} = -\hat{M}^{-1}\mathbf{N}\Delta m$, which means that the gapless point moves as Δm varies and persists even when $\Delta m < 0$, contradicting the initial assumption. Therefore, $\mathrm{Det}\hat{M} = 0$ at the PT point. In fact, the sign of $\mathrm{Det}\hat{M} = \varepsilon_{ijk} M_{1i} M_{2j} M_{3k}$ is the chirality (or chiral charge) of the BTP at $\Delta m = 0$. Since the chirality is a topological number, a BTP with a nonzero chirality is stable against small perturbations. However, when $\mathrm{Det}\hat{M} = 0$, it is not topologically protected. Therefore, when $\Delta m > 0$, the BTP can either be gapped out, leading to another insulating phase, or be split into several Weyl points with zero net chirality, generating a stable metallic phase. When both of these possibilities are allowed, the insulating phase should be preferred since the gapped phase has lower energy.

To understand the nature of the ground state for $\Delta m > 0$, it is useful to rotate the momentum coordinates using a basis which manifests the zero chirality of the BTP at $\Delta m = 0$. Since $\mathrm{Det}\hat{M} = 0$, $\hat{M}$ has an eigenvector $\mathbf{n}_1$ with zero eigenvalue satisfying $\hat{M}\mathbf{n}_1 = 0$. We introduce two additional normalized vectors $\mathbf{n}_2$ and $\mathbf{n}_3$, which can form an orthonormal basis $\{\mathbf{n}_1, \mathbf{n}_2, \mathbf{n}_3\}$, and construct a matrix $\hat{W} = (\mathbf{n}_1, \mathbf{n}_2, \mathbf{n}_3)$. With the rotated coordinate $\mathbf{p} = \hat{W}^{-1}\mathbf{q}$, $\mathbf{f}(\mathbf{p}, \Delta m) = \mathbf{u}_2 p_2 + \mathbf{u}_3 p_3 + \Delta m \mathbf{N}$, where $\mathbf{u}_{2,3} = \hat{M}\mathbf{n}_{2,3}$. Here, terms that are linear in p_1 do not appear in $\mathbf{f}$ due to the fact that $\hat{M}\mathbf{n}_1 = 0$. Then, the leading contribution of the p_1 dependent term should start from quadratic order, which leads to the minimal effective Hamiltonian $H(\mathbf{p}, \Delta m) = \sum_{i=1}^{3} f_i(\mathbf{p}, \Delta m)\tau_i$ in which

$$\mathbf{f}(\mathbf{p}, \Delta m) = \mathbf{u}_2 p_2 + \mathbf{u}_3 p_3 + \mathbf{u}_4 p_1^2 + \Delta m \mathbf{N}. \quad (1)$$

Conditions to obtain an insulator.—Let us first derive the condition for the IIT corresponding to Fig. 1(a). Since the system is gapped for any $\Delta m \neq 0$, the conduction (valence) band should have a well-defined dispersion minimum (maximum) near $\mathbf{p} = 0$. Considering the minimal 2×2 Hamiltonian with $f_{1,2,3}(\mathbf{p}, \Delta m)$ in Eq. (1), the condition to have an extremum for small $\Delta m \neq 0$ leads to the following three equations: $g_i = \partial E_c(\mathbf{p}, \Delta m)/\partial p_i = 0$ ($i = 1, 2, 3$). Here, E_c is the energy of the conduction band. After solving the three coupled equations, the location of the dispersion minimum is obtained as $\mathbf{p}^{\min} = (0, A\Delta m, B\Delta m)$, where A and B are some constants. This implies that, across the ABC, the conduction (valence) band minimum (maximum) should move along the straight line, satisfying $p_1 = 0$ and $p_2 = \frac{A}{B} p_3$ for both $\Delta m < 0$ and $\Delta m > 0$. Such a condition can be satisfied generally when the system has high crystalline symmetry along the line. Therefore, the IIT is achievable when the extrema of the conduction and valence bands of the gapped phases move along a straight line across the ABC.

As a consequence of the IIT, the energy dispersion develops a peculiar structure. To understand the band shape near the dispersion minimum, we compute the Hessian matrix $\hat{H}^{\min}_{ij} = \frac{\partial^2 E_c}{\partial p_i \partial p_j}$, which has a block diagonal form with $\hat{H}^{\min}_{12} = \hat{H}^{\min}_{13} = 0$ at $\mathbf{p} = \mathbf{p}^{\min}$. The other nonzero components of $\hat{H}^{\min}$ satisfy

$$\hat{H}^{\min}_{11} = c_{11}\Delta m, \qquad \mathrm{Det}\begin{pmatrix} H^{\min}_{22} & H^{\min}_{23} \\ H^{\min}_{32} & H^{\min}_{33} \end{pmatrix} > 0,$$

where c_{11} is a constant. Interestingly, $\hat{H}^{\min}_{11}$ changes the sign across the PT because it is linearly proportional to Δm. For $c_{11} < 0$ ($c_{11} > 0$), the conduction band has a dispersion minimum in all three directions for $\Delta m < 0$ ($\Delta m > 0$), while it has a saddle point with a negative curvature along the p_1 direction for $\Delta m > 0$ ($\Delta m < 0$). Therefore when there is a IIT, one insulating phase should possess a saddle point at the bottom (top) of the conduction (valence) band along the p_1 direction where the energy dispersion is quadratic at the QCP.

We can apply this theory to the IIT of the pressured BiTeI [12]. In this system, the ABC occurs along the high symmetry line A-H in the $k_z = \pi$ plane (the BZ of BiTeI is shown in Fig. 1 of Ref. [12]). Because of the C_{3v} symmetry, the conduction (valence) band with Rashba-type spin splitting develops a dispersion minimum (maximum) along this line for any pressure across the ABC, which satisfies the necessary condition for the IIT. In Fig. 2, we plot the evolution of the band dispersion across the ABC near one of the BTPs using the band structure obtained by first-principles calculations [13]. At the QCP, the band dispersion is quadratic along one direction and linear along the other two directions. Moreover, beyond the critical pressure, the band dispersion of the insulating phase possesses a saddle point, proving the occurrence of the IIT.

Conditions to obtain a semimetal.—If the condition for gap reopening is not satisfied, the BTP at $\Delta m = 0$ can be split into several BTPs. Here, we focus on the case of generating two BTPs with opposite chiral charges for convenience. Since there are four parameters ($p_{1,2,3}$ and

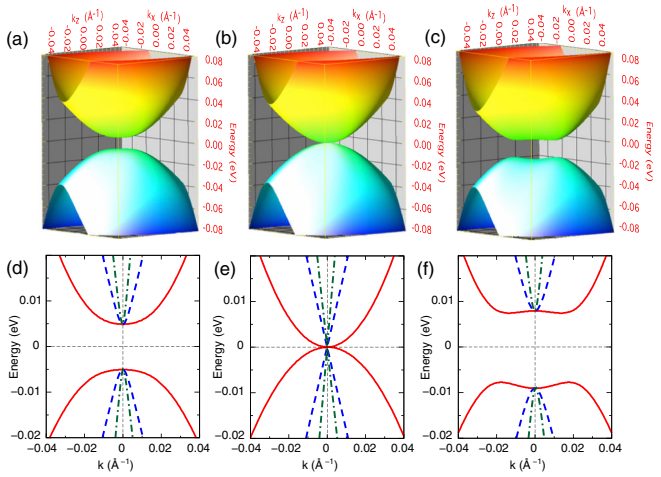

FIG. 2 (color online). Evolution of the band structure, obtained from first-principles calculations, across the topological PT in BiTeI under pressure P. The energy dispersion of the conduction or valence bands near one of the BTPs in the (p_1, p_2) plane, which is normal to the high symmetry line embracing QCPs, is shown for (a) $P < P_c$, (b) $P = P_c$, and (c) $P > P_c$, respectively. Energy dispersions along the p_1 (red solid line), p_2 (green dash-dotted line), and p_3 (blue dashed line) directions are shown for (d) $P < P_c$, (e) $P = P_c$, and (f) $P > P_c$, respectively.

Δm) but only three conditions of $f_{1,2,3} = 0$ are required to be satisfied to achieve a gapless phase, there is a line of gapless points in the $(\mathbf{p}, \Delta m)$ space, in general. Regarding $t \equiv \Delta m$ as a parameter, the trajectories of the two BTPs form a curve $\mathbf{p}^*(t) = (p_1^*(t), p_2^*(t), p_3^*(t))$ in 3D momentum space. To determine the structure of the phase diagram, it is crucial to understand the shape of the curve in 3D space.

When the BTP, $\mathbf{p}^*(t = 0)$, is free of symmetry constraints, the three components of $\mathbf{p}^*(t = 0)$ are linearly independent, in general. In this case, from Eq. (1), the location of BTPs for small $t > 0$ can be obtained as $\mathbf{p}^*(t) = (\pm a_1\sqrt{t}, a_2 t, a_3 t)$ with $a_{1,2,3}$ constants, which is initially proposed by Murakami and Kuga in Ref. [8]. The shape of this trajectory in 3D momentum space and its 2D projections are shown in Fig. 3(a). Since the curve is lying on a 2D plane, the trajectory can form a closed loop, which can generate another insulating state via a pair annihilation of BTPs. Therefore, an ABC at a generic momentum point without symmetry constraints can give rise to Fig. 1(b) [8].

On the other hand, when $\mathbf{p}^*(t = 0)$ is under symmetry constraints, the components of $\mathbf{p}^*(t = 0)$ cannot be linearly independent. For example, in BiTeI, $\mathbf{p}^*(t = 0)$ exists on a line where the Hamiltonian is invariant under the combination of time-reversal and mirror symmetries. Although the IIT should occur in this system, let us suppose that the splitting of the BTP is possible. In this case, it can be shown that the trajectory follows $\mathbf{p}^*(t) = (\pm\alpha\sqrt{t}, \pm\beta t^{3/2}, \gamma t)$ with constants α, β, and γ. This is because the components $p_{1,2,3}$ of $\mathbf{p}^*(t)$ satisfy $p_2 \propto p_1 p_3$ due to the symmetry constraint at $t = 0$. The detailed derivation is provided in the Supplemental Material [14]. The shape of this trajectory is

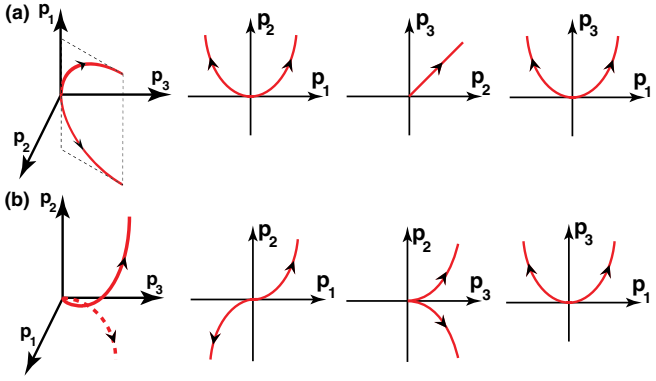

FIG. 3 (color online). The trajectory of BTPs in 3D space and its 2D projections. (a) The curve is lying on a 2D plane leading to Fig. 1(b). (b) The curve is moving in 3D space leading to Fig. 1(c).

shown in Fig. 3(b). It is worth noting that the trajectory moves in 3D space. It is vanishingly improbable that two curves emanating from the origin and traveling in 3D space can collide again, considering the huge volume of the momentum space. Therefore, if an ABC occurs at a momentum under symmetry constraints, the trajectory of BTPs can form an open curve, leading to the phase diagram in Fig. 1(c).

Topological PT.—The IIT can accompany the change of bulk topological properties [15]. In 3D systems with TRS, band insulators can be classified by Z_2 topological numbers $\nu_{0,1,2,3}$ [1,16,17]. In the BZ, there are three pairs of parallel planes, in which $\mathbf{k} \cdot \mathbf{a}_i = 0$ or π $(i = 1, 2, 3)$. Here, $\mathbf{a}_{1,2,3}$ are primitive lattice vectors. Since each plane has TRS, a 2D Z_2 invariant α_i^0 (α_i^π) can be assigned to the plane, satisfying $\mathbf{k} \cdot \mathbf{a}_i = 0$ $(\mathbf{k} \cdot \mathbf{a}_i = \pi)$. Since $\alpha_1^0 + \alpha_1^\pi = \alpha_2^0 + \alpha_2^\pi = \alpha_3^0 + \alpha_3^\pi$, only four 2D invariants are independent and determine the Z_2 invariants of the 3D system in the following way: $(\nu_0, \nu_1, \nu_2, \nu_3) = (\alpha_1^0 + \alpha_1^\pi, \alpha_1^\pi, \alpha_2^\pi, \alpha_3^\pi)$. The strong invariant ν_0 distinguishes a TI $(\nu_0 = 1)$ and a band insulator $(\nu_0 = 0)$. Since $\nu_0 = \alpha_i^0 + \alpha_i^\pi$ for any $i = 1, 2, 3$, if one of the 2D Z_2 invariants changes by 1 through the ABC, a topological PT occurs.

In a 2D BZ with TRS, the Z_2 invariant α is given by the Chern number (modulo 2), which is the integral of the Berry curvature over the half BZ (with additional contraction procedures [16]). Therefore, if the ABC between the valence and conduction bands, changing the Chern number of each band by ± 1 per a touching [18], occurs an odd number of times in the half BZ, α changes by 1, leading to a 3D topological PT. Therefore, when IIT happens, if the high crystalline symmetry line embracing QCPs is on a 2D plane with TRS and the number of such lines in the half BZ is odd, a topological PT occurs. This condition is exactly satisfied in BiTeI, where three high symmetry lines embracing BTPs are on the $k_z = \pi$ plane with TRS leading to the topological PT [12].

Thermodynamic properties at QCP.—The anisotropic dispersion of the BTP with zero chirality leads to the following minimal Hamiltonian at the QCP,

$$H_{\mathrm{QCP}}(\mathbf{p}) = Ap_1^2\tau_1 + vp_2\tau_2 + vp_3\tau_3, \tag{2}$$

where v is the velocity and A is the inverse mass. This gives rise to the density of states $D(\varepsilon) \propto \varepsilon^{3/2}$, which is quite distinct from that for a 3D Weyl semimetal [$D(\varepsilon) \propto \varepsilon^2$] or a 3D normal metal with quadratic dispersion [$D(\varepsilon) \propto \varepsilon^{1/2}$]. The distinct power law of $D(\varepsilon)$ directly leads to new exponents in the temperature dependence of various thermodynamic quantities such as the specific heat (C_V) and compressibility (κ), as summarized in Table I. The diamagnetic susceptibility χ_D also shows an unexpected singular behavior. We have computed χ_D using the Fukuyama formula for the orbital susceptibility $\chi_D = \frac{e^2}{c^2} \times \frac{T}{V}\sum_{n,\mathbf{p}} \mathrm{Tr}[G\gamma_a G\gamma_b G\gamma_a G\gamma_b]$ [19]. Here, G is the Green's function, $\gamma_a \equiv \frac{\partial H_{\mathrm{QCP}}}{\partial p_a}$, and a and b are two orthogonal directions perpendicular to the applied magnetic field. From Eq. (2), χ_D is given by $\chi_D(\theta) = \cos^2\theta\chi_1 + \sin^2\theta\chi_2$, in which $\chi_1 \approx C_1 T^{-1/2}$ and $\chi_2 \approx \chi_2^0 + C_2 T^{1/2}$, with χ_2^0 and $C_{1,2}$ constants. Here, θ is the angle between the external magnetic field and the p_1 direction. Therefore, χ_D shows unusual singular temperature dependence in low temperature, given by $\chi_D \sim T^{-1/2}$ irrespective of magnetic field directions.

Anisotropic dc conductivity.—The anisotropic dispersion at QCP also induces the anisotropic temperature dependence of the dc conductivities. Assuming momentum independence of the scattering rate $\frac{1}{\tau(\omega)}$, a straightforward calculation of the conductivity tensor using the Kubo formula gives rise to the following expression of the dc conductivities:

$$\begin{aligned}\sigma_{11}(T) &= \frac{2e^2\sqrt{A}}{7\pi^2 v^2}\int d\omega|\omega|^{5/2}\left(-\frac{\partial f}{\partial\omega}\right)\tau(\omega),\\ \sigma_{22,33}(T) &= \frac{9e^2}{20\pi^2\sqrt{A}}\int d\omega|\omega|^{3/2}\left(-\frac{\partial f}{\partial\omega}\right)\tau(\omega).\end{aligned} \tag{3}$$

When the Coulomb interaction between electrons dominates the scattering, we can take $\frac{1}{\tau} = \alpha^2 T$, with $\alpha = \frac{e^2}{4\pi\varepsilon v}$, considering that the low temperature transport is dominated by the linear dispersion. In this case, the dc conductivity satisfies $\sigma_{11}(T) \propto T^{3/2}$ and $\sigma_{22,33}(T) \propto T^{1/2}$. On the other hand, when the scattering due to random potentials dominates the transport, using the Born approximation, the leading contribution to the scattering rate can be obtained by $\frac{1}{\tau(w)} \approx 2\pi\gamma_0 D(w)$ with $\gamma_0 = \frac{n_i V_0^2}{2}$ [14]. Here, V_0 is the impurity scattering potential and n_i is the impurity density. Then, using Eq. (3), we obtain $\sigma_{33}(T) = \frac{9e^2v^2}{20\pi\gamma_0}$ and $\sigma_{11}(T) = \frac{2e^2A}{7\pi\gamma_0} \times (2\ln 2)T$, which also shows the anisotropic T dependence [20]. In fact, Eq. (3) implies that, as long as the scattering rate is momentum independent, irrespective of the scattering mechanism, $\frac{\sigma_{11}(T)}{\sigma_{33}(T)} = C_0\frac{A}{v^2}T$, where $C_0 \approx 1.8$.

TABLE I. Temperature (or energy) dependence of various physical quantities for a 3D Weyl semimetal and at the QCP. $D(\varepsilon)$, C_V, κ, χ_D, and σ_{dc} are the density of states, specific heat, compressibility, diamagnetic susceptibility, and dc conductivity, respectively. $\sigma_{\mathrm{dc}}(T)$ is obtained by using the T linear scattering rate due to the Coulomb interaction between electrons.

	$D(\varepsilon)$	$C_V(T)$	$\kappa(T)$	$\chi_D(T)$	$\sigma_{\mathrm{dc}}(T)$
Weyl semimetal	ε^2	T^3	T^2	$\ln T$	T
At the QCP	$\varepsilon^{3/2}$	$T^{5/2}$	$T^{3/2}$	$T^{-1/2}$	$T^{1/2}$

Stability of QCP.—Finally, let us discuss the stability of the QCP against disorder and Coulomb interaction. The effective action of the QCP, including both random disorder potential and $1/r$ Coulomb interaction, can be written as

$$\begin{aligned}S = &\int dtd^3x\Big[\psi^\dagger(i\partial_t + A\partial_1^2\tau_1 \\ &+ \sum_{j=2,3} iv\partial_j\tau_j)\psi + V_i\psi^\dagger M_i\psi\Big] \\ &+ \int dtd^3xd^3x'(\psi^\dagger\psi)_{x,t}\frac{g^2}{2|\mathbf{x}-\mathbf{x}'|}(\psi^\dagger\psi)_{x',t},\end{aligned} \tag{4}$$

where $V_i(\mathbf{x})$ is a random potential coupled to fermion field $\psi(\mathbf{x})$ via a matrix M_i. $g^2 = e^2/\varepsilon$, where e and ε are the electric charge and the dielectric constant, respectively. We take a random disorder potential with Gaussian invariance whose impurity average satisfies $\langle V_i(\mathbf{x})V_j(\mathbf{x}')\rangle = \Delta_{ij}\delta^{(3)}(\mathbf{x}-\mathbf{x}')$. The key characteristic of the Gaussian fixed point in Eq. (2) is the invariance of the Hamiltonian under the anisotropic scaling of spatial coordinates, i.e., $\tilde{x}_1 = x_1/b^{1/2}$ and $\tilde{x}_{2,3} = x_{2,3}/b$, accompanied by $\tilde{t} = t/b$, where the tilde indicates the new scaled coordinates. Under this scale transformation, Δ_{ij} transforms as $\tilde{\Delta}_{ij} = b^{-1/2}\Delta_{ij}$, showing the irrelevance of the disorder. Similarly, we can show that $\tilde{g}^2 = g^2$; i.e., the Coulomb interaction is marginal, which, however, eventually becomes irrelevant, according to the one-loop perturbative renormalization group calculation [21]. Therefore, the unusual power laws in various thermodynamic and transport properties, which are predicted based on the free particle Hamiltonian in Eq. (2), should persist even under the influence of the disorder and the Coulomb interaction.

We greatly appreciate the stimulating discussions with Ammon Aharony, Ora Entin-Wohlman, and Michael Hermele. This work is supported by the Japan Society for the Promotion of Science (JSPS) through the "Funding Program for World-Leading Innovative R&D on Science and Technology (FIRST Program)," and by Grant-in-Aids for Scientific Research (No. 24224009) from the Ministry of Education, Culture, Sports, Science, and Technology (MEXT) of Japan.

[1] L. Fu, C. L. Kane, and E. J. Mele, Phys. Rev. Lett. **98**, 106803 (2007).
[2] X.-L. Qi, T. L. Hughes, and S.-C. Zhang, Phys. Rev. B **78**, 195424 (2008).
[3] S.-Y. Xu *et al.*, Science **332**, 560 (2011).
[4] T. Sato, K. Segawa, K. Kosaka, S. Souma, K. Nakayama, K. Eto, T. Minami, Y. Ando, and T. Takahashi, Nat. Phys. **7**, 840 (2011).
[5] P. Goswami and S. Chakravarty, Phys. Rev. Lett. **107**, 196803 (2011).
[6] H. Isobe and N. Nagaosa, Phys. Rev. B **86**, 165127 (2012).
[7] P. Hosur, S. A. Parameswaran, and A. Vishwanath, Phys. Rev. Lett. **108**, 046602 (2012).
[8] S. Murakami and S.-i. Kuga, Phys. Rev. B **78**, 165313 (2008); S. Murakami, New J. Phys. **9**, 356 (2007).
[9] X. Wan, A. M. Turner, A. Vishwanath, and S. Y. Savrasov, Phys. Rev. B **83**, 205101 (2011).
[10] K. Ishizaka *et al.*, Nat. Mater. **10**, 521 (2011).
[11] M. S. Bahramy, R. Arita, and N. Nagaosa, Phys. Rev. B **84**, 041202(R) (2011).
[12] M. S. Bahramy, B.-J. Yang, R. Arita, and N. Nagaosa, Nat. Commun. **3**, 679 (2012).
[13] Details for first-principles calculations can be found in Ref. [12].
[14] See Supplemental Material at http://link.aps.org/supplemental/10.1103/PhysRevLett.110.086402 for the detailed derivation procedure.
[15] The condition for the topological phase transition mediated by a intervening semimetallic phase can be found in Ref. [8].
[16] J. E. Moore and L. Balents, Phys. Rev. B **75**, 121306(R) (2007).
[17] R. Roy, Phys. Rev. B **79**, 195322 (2009).
[18] M. Oshikawa, Phys. Rev. B **50**, 17 357 (1994).
[19] H. Fukuyama, Prog. Theor. Phys. **45**, 704 (1971).
[20] The T linear behavior of $\sigma_{11}(T)$ due to disorder scattering implies a vanishingly small conductivity in the $T \to 0$ limit. This is an artifact of the simple (non-self-consistent) Born approxiamtion. Once the self-consistency is carefully considered, $\sigma_{11}(T)$ should approach a constant value as $T \to 0$.
[21] B.-J. Yang *et al.* (unpublished).